Journal of Materials Chemistry A

ROYAL SOCIETY OF CHEMISTRY

PAPER

View Article Online
View Journal | View Issue

Check for updates

Cite this: J. Mater. Chem. A, 2023, 11, 5703

Visible-light-driven bistable photoswitching with enhanced solid state NIR-fluorescence for multi-level optical storage†

Pan Hong,[a] Nuo-Hua Xie,[ab] Kai Xiong,[a] Jing Liu,[a] Ming-Qiang Zhu[a] and Chong Li*[a]

Received 9th December 2022
Accepted 6th February 2023

DOI: 10.1039/d2ta09607b

rsc.li/materials-a

Photoswitchable near-infrared (NIR) fluorescence molecules have the characteristic of reversible NIR luminescence modulation, showing broad application prospects in advanced photonic applications such as optical storage and super-resolution fluorescence imaging. Herein, a visible-light-driven solid-state NIR fluorescent bistable molecular switch TDI-4(DTE-TPE) was constructed by covalently coupling aggregation-induced emissive tetraphenylethylene (TPE), photochromic dithienylethene (DTE) and NIR emissive terrylene diimide (TDI) into a single molecule. As the bulky TPE groups hinder the molecules from stacking, the open-form TDI-4(DTE-TPE) exhibits enhanced NIR in the solid state with a maximum emission wavelength of 786 nm, whose fluorescence intensity is 35 times higher than that of its precursor TDI powder. Upon 405 nm visible light irradiation, the open form converted into non-fluorescent closed form, accompanying a fluorescence quenching of >93%, arising from the electron-donating conjugation ability of the TPE group. This process is reversible under another longer wavelength irradiation with excellent fatigue resistance. Also, both the open and closed forms were stable at 85 °C and 85% humidity in air for more than 1000 h, showing great bistability and aging resistance. Benefitting from these, its PMMA film realizes multi-level optical information storage, which is a promising photonic storage medium.

Published on 07 February 2023. Downloaded on 12/4/2025 7:14:57 PM.

1 Introduction

Low-energy long-term secure storage of massive data is increasingly arousing concerns in the era of big data we are entering.[1,2] Optical storage is considered to be an important alternative for massive data storage with competitive energy saving and long-term safety in the future.[3] However, at present, the size of the traditional optical storage unit is close to its limits. It is of great significance to develop higher density, larger capacity optical storage mediums, and technologies. At present, the technologies to improve the optical data storage density mainly include three-dimensional (3D) or multi-layer storage,[4] super-resolution storage,[5] and multi-level storage.[6] Among them, the 3D storage and super-resolution technology rely strongly on complicated or expensive devices. Instead, a multi-level strategy is a more direct and effective route to achieve high-density optical storage, and it is also a basic technology that can be combined with 3D and super-resolution ones.

Photoswitchable fluorescent molecules are photochromic materials working at the single-molecule level and are sensitive to light irradiations to generate reversible changes in physical properties and can be utilized for optical information storage, such as programmable patterning,[7] anti-counterfeiting[8] and high-density data storage.[4] Photon-model recording technology based on photochromic materials shows great promise for high-density data storage.[9] Initially, photoswitchable absorption changes (color, reflectivity changes, *etc.*) were employed for multi-level optical storage.[10] In recent years, photochromic materials with fluorescence photoswitching functions have been developed rapidly.[11–13] Compared with the absorption signal, the fluorescence signal has higher detection sensitivity and limit, and also the feasibility of non-destructive readout.[14–18] Therefore, molecular photoswitches with optically controlled fluorescence switching capacity show more broad application prospects in photon-model storage. Moreover, photoswitchable fluorescence molecules with high switching contrast and robust bistability are expected to achieve multi-level fluorescence signals with greatly increased storage density. However, the current research of optical storage based on photoswitchable fluorescence molecules is mainly focused

[a]Wuhan National Laboratory for Optoelectronics, School of Optical and Electronic Information, Huazhong University of Science and Technology, Wuhan 430074, China. E-mail: chongli@hust.edu.cn

[b]Jingdezhen Ceramic University, School of Materials Science and Engineering, Jingdezhen 333403, China

† Electronic supplementary information (ESI) available. See DOI: https://doi.org/10.1039/d2ta09607b

Published on 07 February 2023. Downloaded on 12/4/2025 7:14:57 PM.

on conventional binary data recording, while their multi-level fluorescence storage has not yet been reported.

Compared with other types of photoswitchable molecules, diarylethene shows these main outstanding advantages: (1) diarylethene has unique bistable states, which is the basic guarantee for stable information recording; (2) its excellent fatigue resistance can guarantee long-term repeatable data reading, writing, and erasing; (3) it keeps eminent photoswitching performance in rigid media, which makes them competent in optoelectronic devices.[19–21] Photoswitchable fluorescence diarylethene is one of the most promising photochromic optical storage media[8] but faces the problem of fluorescence signal destructive readout.[22] How to realize the non-destructive readout of fluorescence signals is an important question.[23] Recently, near-infrared (NIR) fluorescent materials have been widely applied in bio-imaging and optoelectronic devices due to their large penetration depth, low background, little light interference, and chemical adjustability of molecular structure.[24,25] By utilizing the fact that the NIR fluorescent wavelength is far away from the absorption wavelength of the photoswitching unit and taking the photo-induced electron transfer (PET) mechanism to quench the fluorescence of closed-form NIR fluorescent diarylethenes at the same time, the nondestructive readout of the fluorescence signal was accomplished.[26,27] It indicated the photoswitchable NIR diarylethenes are promising optical storage media for practical applications.

However, photoswitchable NIR-fluorescence molecules have not been widely studied due to the difficulty of molecular design to a great extent. Decorating NIR-fluorescence groups on photochromic diarylethene is a common strategy to construct photoswitchable NIR fluorescent diarylethene molecules. For example, NIR fluorophores, such as porphyrins,[28] benzothiadiazole-derivative,[24] cyanine dyes,[29,30] cyanovinylene-backboned conjugated polymers,[31] transition metal[32] or lanthanide complex,[14] PdS nanocrystal,[33] terrylene diimide (TDI),[34] have been introduced in diarylethene systems recently, making great progress on NIR fluorescence photoswitching. Among them, TDI is the higher rylenediimides similar to perylene diimides (PDI),[35] which possesses outstanding optical properties, such as high fluorescence quantum yield, large molar extinction coefficient, and outstanding photostability.[36] The Würthner's group[34] first introduced stable and bright NIR fluorescent TDI on the two sides of diarylethene units to form NIR fluorescent photoswitching for non-destructive readout, which can work in some polar solvents. In our previous work,[16] the photochromic diarylethene was connected to the TDI to obtain a photoswitchable NIR fluorescent molecules with a high 'ON/OFF' switching contrast upon 302 nm UV irradiation. As the NIR emission spectrum of TDI and the absorption spectrum of closed-form diarylethene only partially overlapped, the 'quasi' non-destructive readout of fluorescence was realized for non-volatile optical memory applications.

In practical application scenarios, the required materials often exist in the form of solid, film or highconcentration/density state.[37] However, most of the present NIR fluorescent diarylethenes were investigated under low-concentration solutions rather than the solid state.[34] Like the conventional NIR fluorescent dyes, NIR fluorescent diarylethenes also meet the problems of weak NIR emission and serious aggregation-caused quenching (ACQ) phenomenon, which significantly limits its application in bio-imaging and optoelectronic devices. Furthermore, these photoswitchable NIR-fluorescence diarylethenes generally require high-energy UV light to drive the photocyclization reaction.[24] As is known, UV light has a strong light damage effect and relies on expensive instruments, which is desirable to be resolved. Therefore, the development of visible-light-driven photoswitchable solid-state NIR fluorescent diarylethene is of great significance.[38]

In order to simultaneously achieve enhanced solid-state NIR fluorescent, all visible-light driving photoswitching and large ON/OFF switching ratio, we introduced four tetraphenylethylene (TPE)-modified dithienylethene (DTE) groups at the TDI bay-positions to prepare a novel visible light-driving solid-state high-brightness NIR fluorescent diarylethene TDI-4(DTE-TPE). In this system, TDI provides a near-infrared emission function. DTE provides the photochromic function. The quadruple DTE groups substitution strategy can dramatically improve the fluorescence ON/OFF switching ratio. TPE can effectively increase the conjugation of the whole molecule, promoting the red shift absorption and thereby the visible light sensitivity of DTE photoswitching units. At the same time, TPE has a propeller-like aggregation-induced emission (AIE) structure with large steric hindrance, which could effectively inhibit the strong intermolecular π–π stacking to weaken the non-radiative decay of the excitation state and thereby increase the solid-state NIR fluorescence. As expected, TDI-4(DTE-TPE) molecule exhibits all-visible-light controlled NIR fluorescent, achieving a considerable fluorescence switching ratio under 405 nm light. Based on the great visible light responsibility and solid-state NIR fluorescence, the application for multi-level optical information storage was demonstrated.

2 Results and discussion

2.1 Molecular design, synthesis, characterizations

The synthesis of TDI-4(DTE-TPE) looks challenging at first glance due to its large molecular structure. Herein, we adopted the idea of building blocks to achieve highly efficient synthesis. Firstly, TDI moiety bearing four borate ester groups[39] and DTE moiety with monobromo decoration[40] were synthesized. Then, they can be coupled by a highly efficient Suzuki cross-coupling reaction to afford TDI-4(DTE-TPE) with a yield as high as 64.2%. The molecular structure of TDI-4(DTE-TPE) is shown in Scheme 1. Its detailed synthesis route and characterizations are described in the ESI.† Its purity was tested to be 98.9% by high-performance liquid chromatography (HPLC) (Fig. S1†). Its molecular ion peak measured by MALDI-TOF is 3990.55 for $[M + 1]^+$, well consistent with the theory value 3990.01 (Fig. S2†). The above results are in full agreement with the structure of the target product TDI-4(DTE-TPE).

The AIE-active TPE group in the molecular structure of TDI-4(DTE-TPE) has a large steric hindrance effect. Four bulky TPE-DTE groups are covalently connected to a single TDI fluorophore through the oxygen-atom bridge bonds.[39] This not only

 This journal is © The Royal Society of Chemistry 2023

Published on 07 February 2023. Downloaded on 12/4/2025 7:14:57 PM.

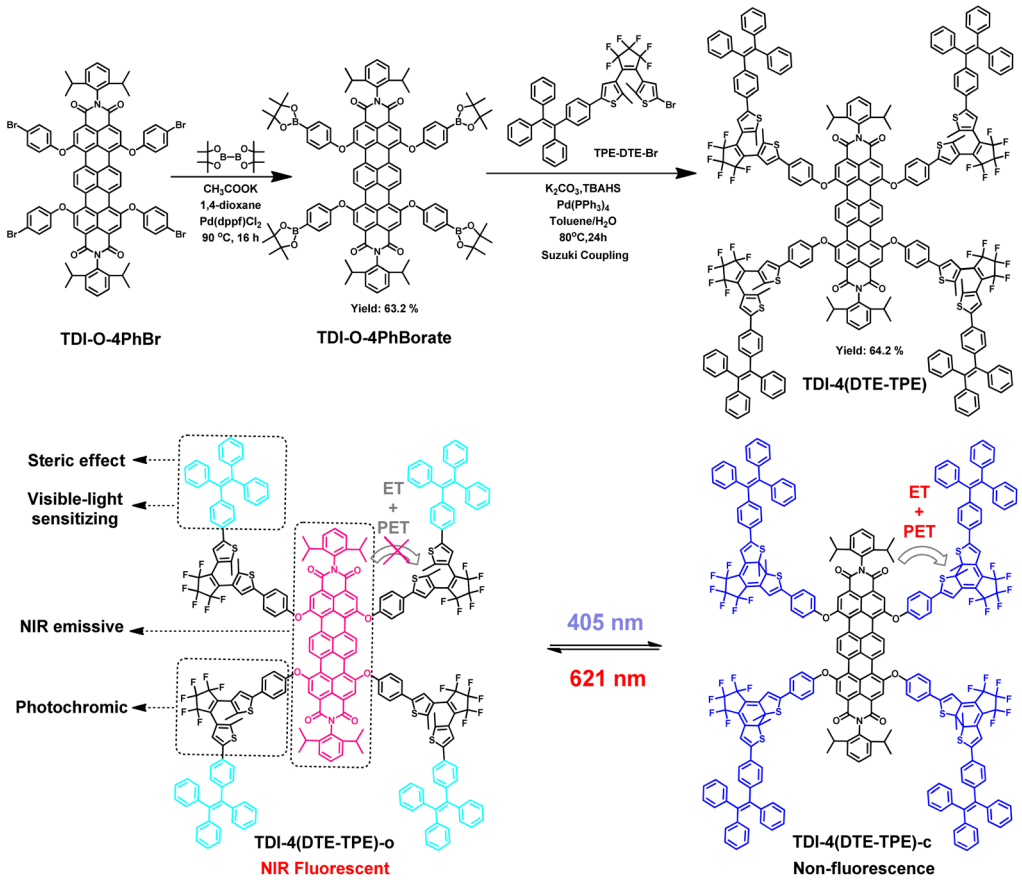

Scheme 1 The synthesis route, chemical structures and photochromic reactions of TDI-4(DTE-TPE). PET means the photo-induced charge transfer, ET means the energy transfer.

preserves the individual optical properties of the two structural parts but also avoids the strong π–π stacking interactions between the TDI cores such as the H-aggregation[41–43] and excimers[44–47] which could quench the fluorescence. Thus the non-radiative decay of excitons was weakened, resulting in bright NIR emission in the aggregate or solid state. On the other hand, TPE has good electron-donating conjugation capacity and effectively extends the conjugation of DTE moiety to achieve visible-light driving ability.[48–50] The introduction of TPE groups has the effect of 'two birds with one stone', while the quadruple diarylethene substitution strategy can dramatically improve the ON/OFF contrast of the fluorescent photoswitching.

2.2 Photochromic property

TDI-4(DTE-TPE) molecule can realize visible light-driven photocyclization reaction as expected. The photochromic properties of its tetrahydrofuran (THF) solution and polymethyl methacrylate (PMMA) film under 405 nm visible light irradiation are shown in Fig. 1. The absorption spectra of TDI-4(DTE-TPE) resembles the combination of that of its moieties model compounds in both open-form and closed-form cases (Fig. S3b and d†). The open-form TDI-4(DTE-TPE) (abbr. TDI-4(DTE-TPE)-o) sample is green in color (Fig. S4†). Its maximum absorption peaks at 608 nm and 663 nm are from the TDI moiety as open-form DTE moieties usually do not have absorption at that long wavelength, which is also consistent with the computed energy gap of 1.87 V (Fig. S5†). The other absorption peak at ∼300 nm is mainly contributed by the open-form TPE-DTE group (Fig. S3b†). Upon 405 nm visible light irradiation, the DTE unit undergoes the photocyclization reaction, *i.e.*, the open form DTE is converted to the closed form one (TDI-4(DTE-TPE)-c). The solution becomes blue in color, accompanying the sharply rising absorption at ∼605 nm, which is ascribed to the forming of closed-form DTE (Fig. S3c and S6†). After 80 s 405 nm irradiation, the photostationary state (PSS) was reached and the absorption did not change anymore. Using other long wavelengths of visible light irradiation (*e.g.* 621 nm), it recovered to the initial open form state. Upon UV or short wavelength light irradiation, the open-form DTE can be partially converted to the closed-form one. The situation is different for the long wavelength visible light irradiation on the closed-form DTE. Although the photocycloreversion quantum yield is low, the photocycloreversion reaction would be complete as only the closed-form DTE can absorb the long wavelength visible light rather than the open-form one (Fig. S3†). Thus, only the ring-opening reaction could happen under long-wavelength visible-light irradiation. That is to say the closed form DTE can be turned to the full open form DTE (*i.e.*, TDI-4(DTE-TPE)-o) upon

Published on 07 February 2023. Downloaded on 12/4/2025 7:14:57 PM.

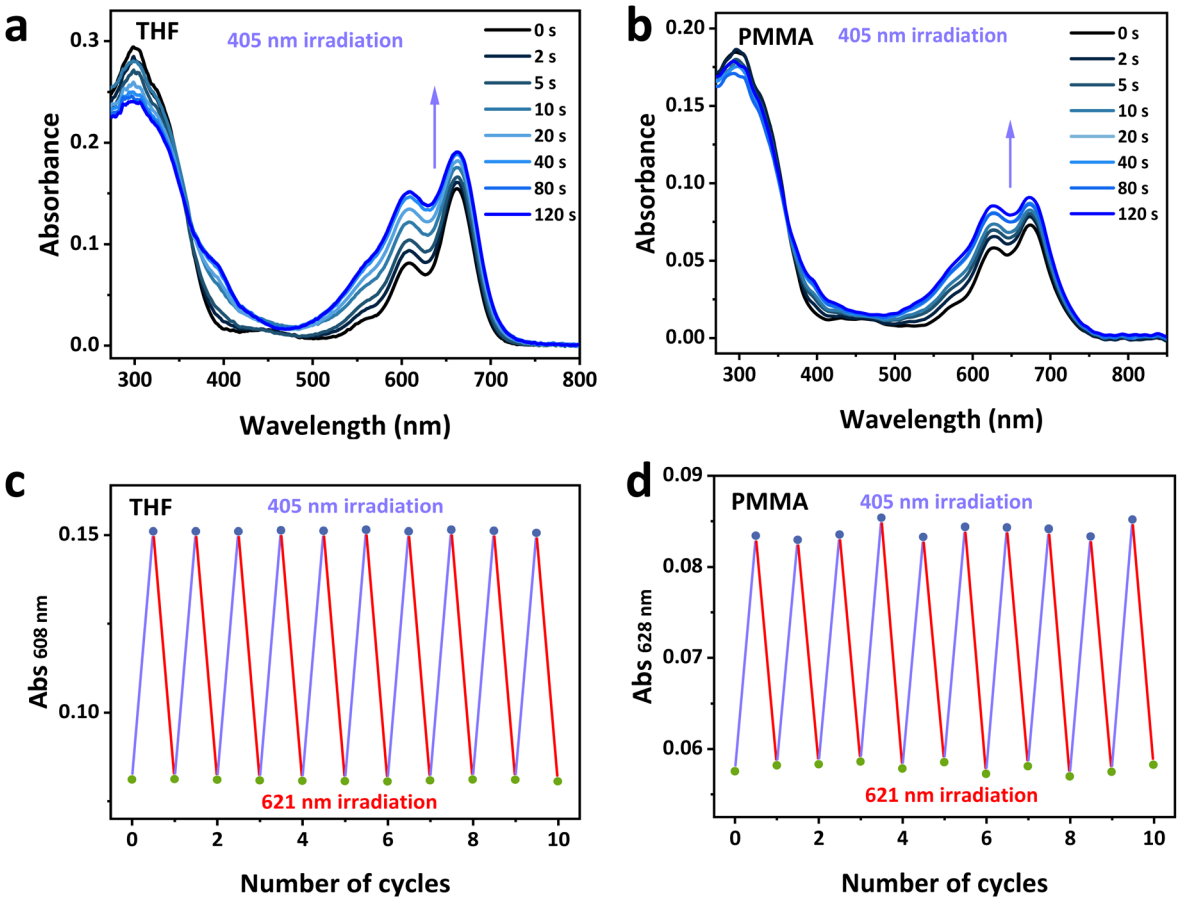

Fig. 1 The photochromic properties of TDI-4(DTE-TPE) in THF solution (1×10^{-6} M) and PMMA film (2 wt%) under visible light irradiations. The absorption spectra changes of TDI-4(DTE-TPE) in (a) THF solution and (b) PMMA film upon 405 nm visible light irradiation. (c) The first 10 photoswitching cycles of the absorbance at 608 nm of TDI-4(DTE-TPE) in THF solution under alternating irradiations of 405 nm (40 s) and 621 nm (5 min) lights. (d) The first 10 photoswitching cycles of the absorbance at 628 nm of TDI-4(DTE-TPE) PMMA film under alternating irradiations of 405 nm (80 s) and 621 nm (8 min) lights.

relatively longer wavelength irradiation (such as 621 nm, 589 nm and 550 nm, see Fig. S7†). Experimentally, it takes about 180 s for the complete photocycloreversion reaction to achieve the full open form DTE (Fig. S8 and S9†), For the photoswitching cycles test, we used a longer irradiation time of 5 or 8 min to guarantee the full open form state. Upon alternating irradiations of 405 nm violet-blue and 621 nm red lights (Fig. 1c and d), the above processes can be repeated at least 10 times with negligible absorption changes of both open- and closed-form TDI-4(DTE-TPE), exhibiting considerable photochromic reversibility and fatigue resistance. The change of ^{1}H NMR spectra of TDI-4(DTE-TPE) with the increased irradiation times of 302 nm UV light and 405 nm visible light, respectively, was monitored (Fig. S10†). By calculating the integral area ratio of the methyl groups on thiophene rings 2.13 ppm (open-form DTE) and 1.93 ppm (closed-form DTE) peaks,[39] the conversion yields from the open-form DTE to the closed one at PSS at 302 nm and 405 nm were 95.8% and 49.3%, respectively. The photoisomerization quantum yields were tested based on the dynamic absorption results (Fig. S11–S13†) according to the reported method.[39] The photocyclization quantum yields $\Phi_{o\rightarrow c}$ at 302 nm and 405 nm irradiations were 0.42 and 0.12, respectively. The photocycloreversion quantum yields $\Phi_{c\rightarrow o}$ at 621 nm was 0.013, which is comparable to the results obtained on a similar dithienylethene core structure from the literature.[39,51,52] It indicates that TDI-4(DTE-TPE) has a moderate 405 nm visible light responsiveness and excellent ultraviolet light responsiveness.

2.3 Solid-state NIR fluorescence performance

TDI-4(DTE-TPE)-o contains the NIR fluorescent TDI group. In low polar solvents, there is a bright NIR emission with a fluorescence quantum yield (FLQY) of 0.52 in cyclohexane (Table S1†). The maximum emission wavelength is 701 nm in dilute THF solution (FLQY = 0.46). The NIR emission decreased in high polar solvents along with a red shift of emission peak (Fig. 2b). This is probably caused by a bit distorted donor–π–acceptor (D–π–A) structure of the TDI core with four –O– bridges.[49] When the solvent polarity is high, the intramolecular charge transfer (ICT)[53] is intensified to accelerate the non-radiative transition process. As a result, the fluorescence emission is weakened in the polar solvent. The FLQY of TDI-4(DTE-

 This journal is © The Royal Society of Chemistry 2023

Published on 07 February 2023. Downloaded on 12/4/2025 7:14:57 PM.

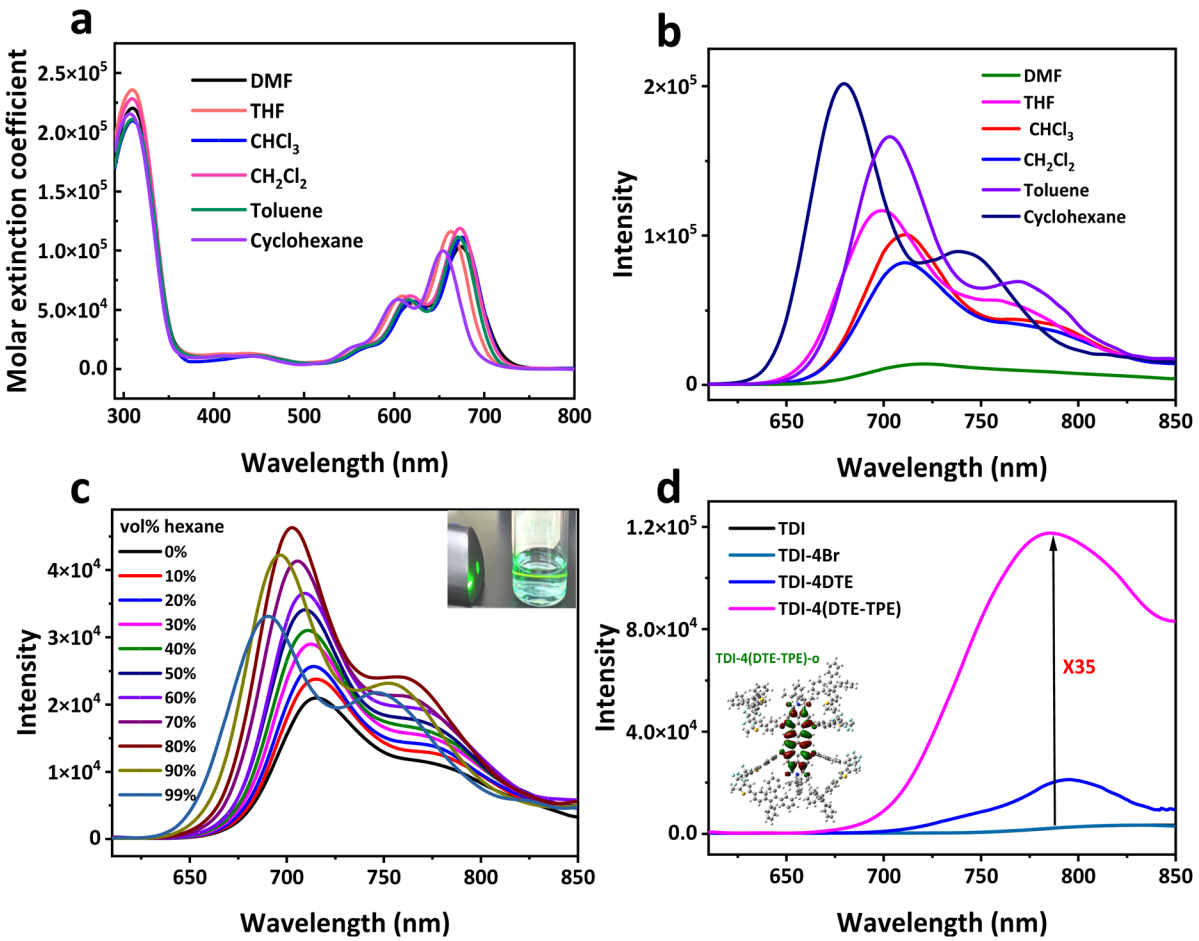

Fig. 2 NIR fluorescence properties of TDI-4(DTE-TPE). (a) The molar extinction coefficient and (b) fluorescence spectra of TDI-4(DTE-TPE) in different solvents. (c) The fluorescence spectra of TDI-4(DTE-TPE) in the dichloromethane–hexane binary solvent with different volume percentages of *n*-hexane. The insert is the Tyndall effect test result of the sample in 99% hexane by a green laser. (d) The solid state emission spectra of TDI, TDI-4Br, TDI-4DTE (their molecular structure was shown in Fig. S13†), and TDI-4(DTE-TPE) with the same equipment parameters. The concentrations of the solution samples are all 5×10^{-6} M. The excitation wavelength for the fluorescence test is 600 nm.

TPE) in cyclohexane is 2.7 times that in dichloromethane (DCM).

Due to its large planar conjugated structure, TDI's simple derivatives are prone to form strong H-aggregation and excimers between the molecules to quench the fluorescence.[41–43,45–47] Therefore, the fluorescence emission of TDI derivatives (*e.g.*, TDI and TDI-4Br in Fig. 2d) in the solid state or high concentration is usually very weak. Given this, we introduced a sterically hindered bulky structure of propeller-like TPE groups surrounding the TDI core, expecting to impair the stacking effect to achieve enhanced solid-state NIR fluorescence. In order to verify the fluorescence enhancement phenomenon caused by its steric effect, we carried out AIE performance test experiments on TDI-4(DTE-TPE)-o. We chose DCM-hexane binary solvent to study its aggregation-induced luminescence property (Fig. 2c). With the increase fraction of the poor solvent hexane in the DCM solution of TDI-4(DTE-TPE)-o, it maintained a uniform, stable and transparent liquid. The fluorescence intensity of TDI-4(DTE-TPE) increases steadily with the increase of the hexane fraction value f_{hex} till it reaches 80%. After f_{hex} is greater than 80%, the fluorescence intensity decreases slightly with a slight blue shift of emission peak from 716 nm to 691 nm. This is possibly caused by the ordered aggregation of molecules to form nanoparticles when the f_{hex} is large enough.[54] When f_{hex} is 99%, the Tyndall effect was obvious Fig. S14,† evidencing that TDI-4(DTE-TPE) molecules form nanoparticles which were further confirmed by TEM (Fig. S15†). Nevertheless, in this aggregation state, the FLQY is still 1.8 times that in DCM (Table S1†). This is probably attributed to the bulky DTE-TPE moieties to prevent the serious aggregation of TDI cores.

TDI-4(DTE-TPE) was also expected to exhibit enhanced NIR emission in the solid or condensed state. Its solid-state emission spectrum is compared with that of its analogues TDI, TDI-4Br, and TDI-4DTE (Fig. 2d and S16†). The NIR fluorescence of large planar molecules TDI and TDI-4Br without bulky substituents is extremely weak in the solid powder state due to the strong π–π stacking interaction.[55] TDI-4DTE with bulky DTE substituents has improved solid-state NIR fluorescence, but much less than that of TDI-4(DTE-TPE). That is because TDI-4(DTE-TPE) is a highly bulky three-dimensional molecular

Published on 07 February 2023. Downloaded on 12/4/2025 7:14:57 PM.

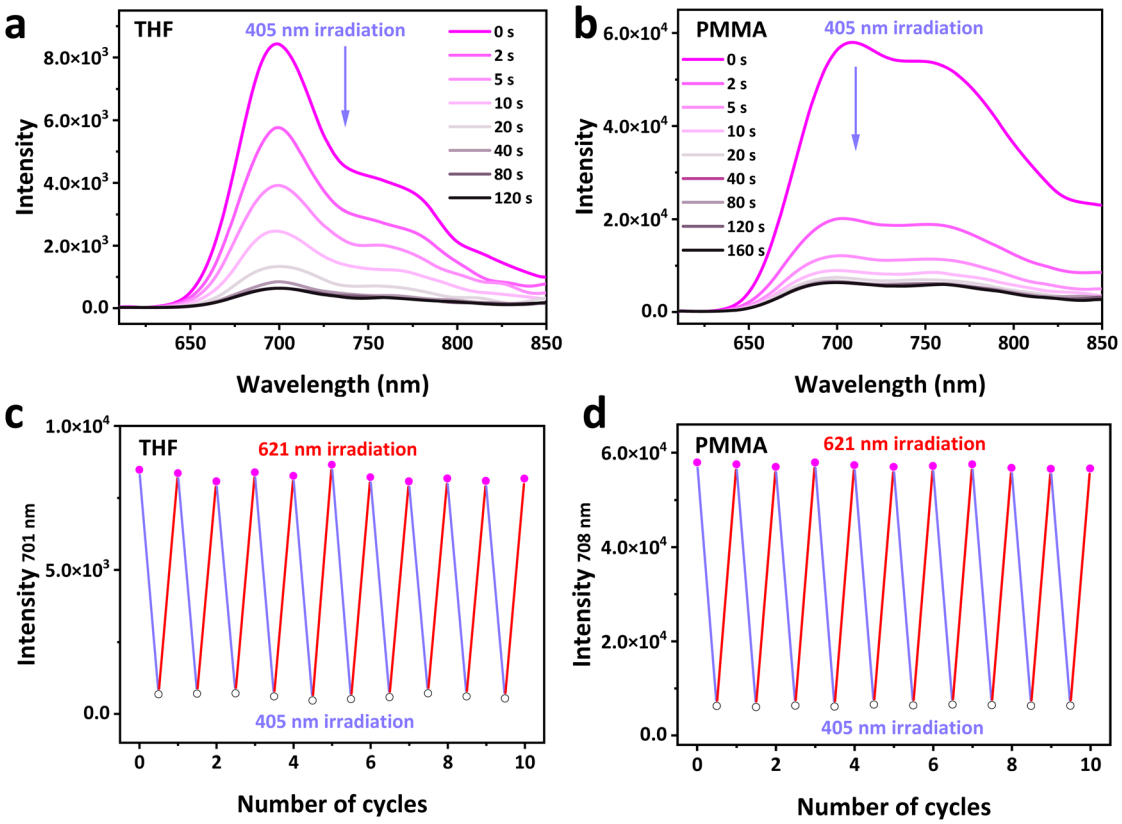

Fig. 3 The NIR fluorescence photoswitching properties of TDI-4(DTE-TPE) in THF solution (1×10^{-6} M) and PMMA film (2 wt%) under visible light irradiations. The fluorescence spectra changes of TDI-4(DTE-TPE) in (a) THF solution and (b) PMMA film upon 405 nm visible light irradiation. (c) The first 10 photoswitching cycles of the fluorescence intensity at 701 nm of TDI-4(DTE-TPE) PMMA film under alternating irradiations of 405 nm (40 s) and 621 nm (5 min) lights. (d) The first 10 photoswitching cycles of the fluorescence intensity at 708 nm of TDI-4(DTE-TPE) PMMA film under alternating irradiations of 405 nm (80 s) and 621 nm (8 min) lights. The excitation wavelength for fluorescence spectra is 600 nm.

structure, in which the TPE-DTE group is wrapped to the TDI core (Fig. S17†). It shows that TDI-4(TPE-DTE) powder is more like an amorphous state as no obvious XRD peaks were observed (Fig. S18†). TDI-4(DTE-TPE) molecules tend to be more loosely packed in the solid state with a lowered intermolecular π–π interaction. Nevertheless, the amorphous TDI-4(TPE-DTE) solid powder still results in the formation of molecular excimers, which can be deduced from a red shift of emission in solid state compared to the monomer emission in solutions and the lack of vibronic peaks in this red-shifted emission[45–47] (Fig. 2b and d). In contrast, there are abundant peaks in the XRD spectrum of the TDI-4Br powder (Fig. S18†). It means that as a simple TDI derivative, TDI-4Br powder has regular molecules stacking in short- or long-range orders. The interplanar distance of TDI-4Br molecules in the power state was estimated to be about 3.76 Å according to the literature method,[47] which further supports the excimer and H-aggregation quenching mechanism of the TDI core. The result indicates that TDI-4(TPE-DTE) did not form orderly stacking structures, which is an evidence of the bulky structure restraining the π-stacking when considering the above result of its analogue TDI-4Br. As a result, it has relatively strong NIR emission at a solid state with a maximum emission wavelength of about 786 nm located in the typical first NIR region. Compared with TDI, the maximum fluorescence intensity of TDI-4(DTE-TPE) solid powder is increased by 35 times. In general, TDI-4(DTE-TPE) exhibits enhanced NIR emission in the aggregation state and solid state. The introduction of four bulky TPE-DTE groups improves the solid-state NIR fluorescence performance, which makes TDI-4(DTE-TPE) more suitable for solid-state applications than TDI-4DTE.

2.4 Fluorescence photoswitching performance

As TDI-4(DTE-TPE) contains photochromic DTE groups, it shows a fluorescence photoswitching function. Besides UV light irradiation (Fig. S12 and S13†), short wavelength visible light such as 405 nm can also induce fluorescence quenching (Fig. 3 and S19†). The band gap of the open-form DTE moieties (DTE-o) is larger than that of TDI, and the energy transfer from the excited TDI core to DTE-o will not take place.[16] Meanwhile, the energy levels of the DTE-o do not match the LUMO level of TDI (Fig. S20†) to induce the photoinduced electron transfer (PET) between them.[35] Therefore, the TDI-4(DTE-TPE)-o exhibits a bright NIR fluorescent state. Upon 405 nm visible light irradiation, the TDI-4(DTE-TPE)-c is generated accompanying the quenching of NIR fluorescence. A photostationary state (PSS) was achieved after less than 80 s of 405 nm irradiation in THF

 This journal is © The Royal Society of Chemistry 2023

Published on 07 February 2023. Downloaded on 12/4/2025 7:14:57 PM.

solution (Fig. 3a). The maximum fluorescence quenching efficiency was more than 93% and the on-off switching ratio was 14 : 1 (Table S2†). The quenching mechanism of TDI-4(DTE-TPE)-c is described below. First, the energy band gap of the closed-form DTE moiety (DTE-c) is still higher than that of the TDI moiety (Fig. S20†). The fact that the absorption spectrum of DTE-c poorly overlaps with the TDI fluorescence spectrum also confirms it (Fig. S3a†), indicating a low probability of the energy transfer between them. Thus, PET is prone to occur as the energy levels of DTE-c match well with that of TDI (Fig. S20†),[34,56] which can efficiently cause the NIR fluorescence quenching of TDI. Thus, TDI-4(DTE-TPE)-c is in a non-fluorescent state. The initial fluorescent state was restored after applying another long wavelength of visible light irradiation (*e.g.* 621 nm) (Fig. 3c and d). Showing the same steps with the absorption spectra (Fig. S8†), the fluorescence intensity of the closed-form TDI-4(DTE-TPE)-c was increased upon a relatively long wavelength light irradiation till reaching a plateau, where it is actually the initial open-form TDI-4(DTE-TPE)-o, in about 3 min (Fig. S9†). Upon alternating 405 nm and 621 nm light irradiations, TDI-4(DTE-TPE) undergoes reversible NIR fluorescence switching in the THF solution (Fig. 3c). After 10 cycles, the NIR fluorescence loss does not exceed 5%, which once again proves the great fatigue-resistance performance of TDI-4(DTE-TPE). The fluorescence switching performance of TDI-4(DTE-TPE) in PMMA film is a little lower than that in the solution state (Fig. 3b). In PMMA film, the maximum fluorescence quenching efficiency and ON/OFF switching ratio were 90% and 9.5 : 1 at the photostationary state (405 nm irradiation for 80 s), respectively. It also showed excellent fatigue resistance in the solid PMMA film (Fig. 3d). TDI-4(DTE-TPE)'s remarkable performance on NIR fluorescence photoswitching laid a foundation for its application in optical storage and other fields.

2.5 Multilevel optical storage

The NIR-fluorescence and non-fluorescent states of a single TDI-4(DTE-TPE) molecule can be regarded as the binary digits of '0' and '1', respectively. In practice, one data recording unit usually has a size larger than the light diffraction limit, which is actually a crowd of molecules. Thus, the proportion of molecules undergoing photoisomerization can be strictly related to the dose of light irradiation. Employing this principle, multi-level signal amplitude control for recording information could be realized based on photoswitchable fluorescent materials. By controlling the exposure dose of the writing light (power × time), the maximum NIR-fluorescence ON/OFF switching contrast (*i.e.* signal amplitude) can be divided into several signal steps to achieve multi-level storage. In this work, TDI-4(DTE-TPE) molecules were doped within polymethyl methacrylate (PMMA) and then this mixture sample was spin-coated on a quartz wafer to prepare an optical storage media film. For optical storage applications, the reliability and durability of the storage media are important factors.[57] For this, we first performed an aging test at 85 °C temperature and 85% humidity on both the open-form and closed-form TDI-4(DTE-TPE) films. After 1000 hours of aging, the TDI-4(DTE-TPE) film seems hardly changed from the absorption and fluorescence spectra before and after the aging test (Fig. 4). The results prove that the material has good bistability and anti-aging performance.

Subsequently, the TDI-4(DTE-TPE) film was applied for multi-level storage (Fig. 5a). As the proof of the principle

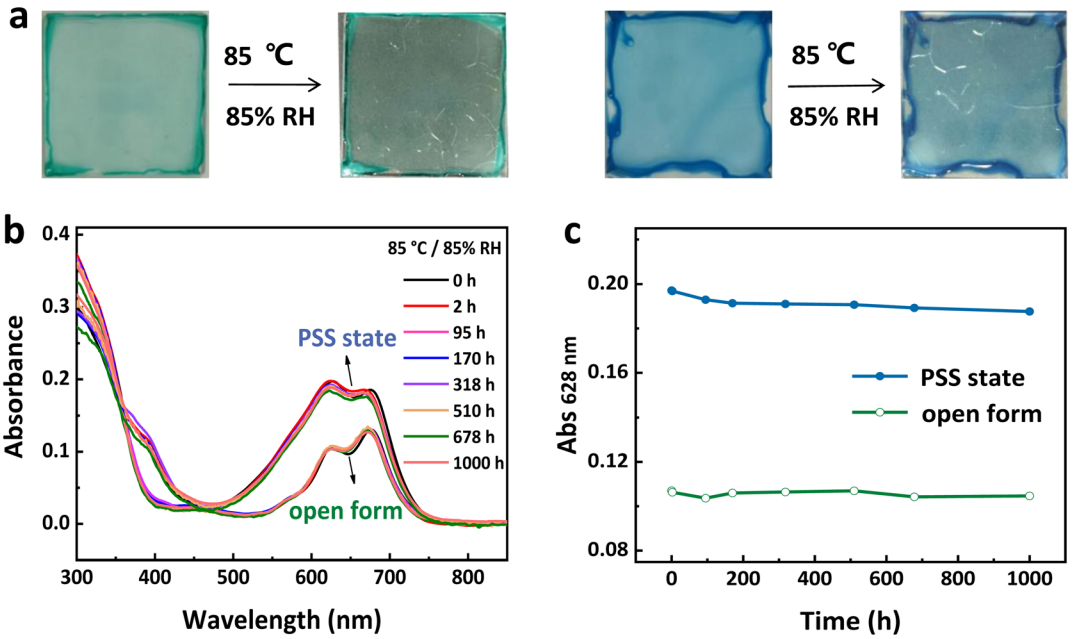

Fig. 4 The aging test for the TDI-4(DTE-TPE) in PMMA for 1000 h at 85 °C and 85% humidity. (a) The photos of the open-from (left side) and photostationary-state (PSS at full 302 nm irradiation, right side) TDI-4(DTE-TPE) PMMA film before and after the aging test. The monitoring of (b) the absorption spectra and (c) the absorbances at 628 nm of the open-form and photostationary state (PSS at full 302 nm irradiation) samples during the aging test.

Published on 07 February 2023. Downloaded on 12/4/2025 7:14:57 PM.

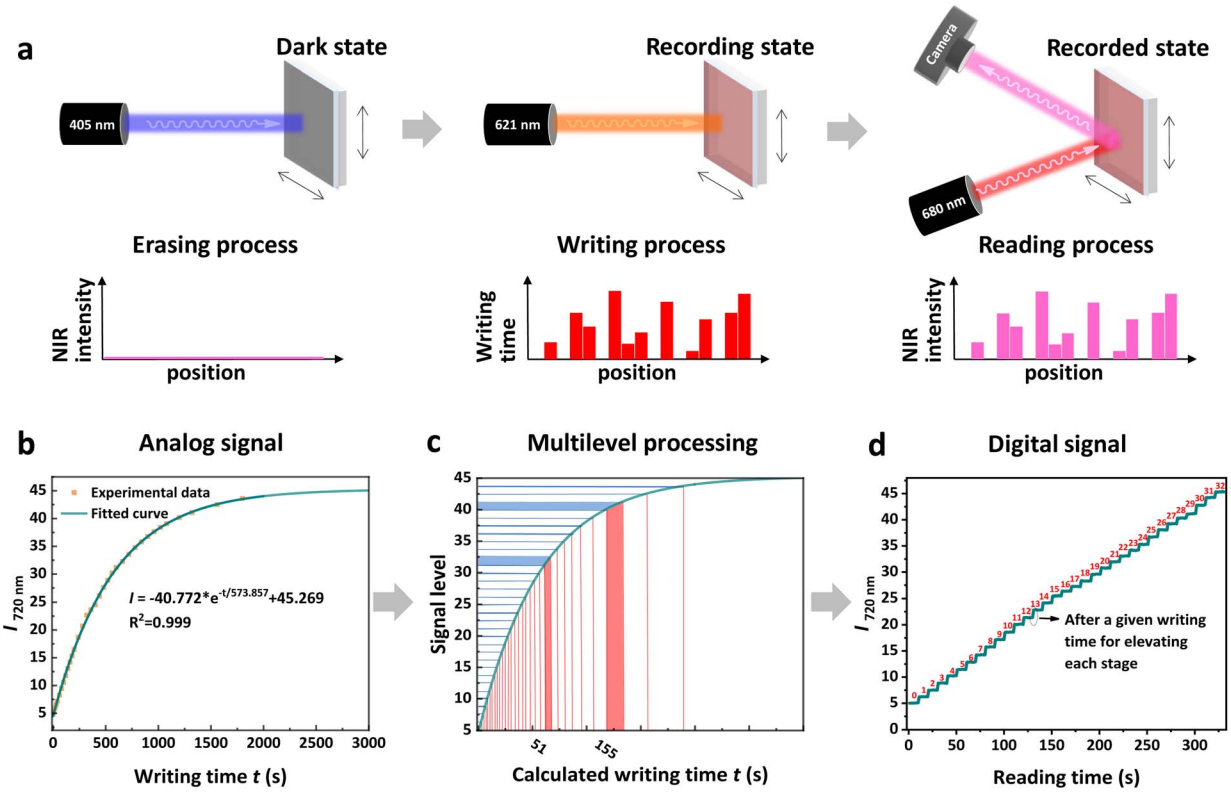

Fig. 5 Multi-level optical storage principle and model based on TDI-4(DTE-TPE) PMMA film. (a) The schematic processes of multi-level optical storage, the recording process was started from a dark state sample, which was irradiated by 405 nm irradiation (*i.e.*, erasing process). The NIR intensity at 720 nm was related to the time of 621 nm writing light irradiation. The information (with the form of fluorescence intensity at 720 nm) could be erasable stored and accessed under 405 nm (erasing), 621 nm (writing), and 680 nm (reading) illuminations. (b) The fluorescence intensity of TDI-4(DTE-TPE) PMMA film varied with the exposure time of a writing light (621 nm). The experiment data were fitted well with a single exponential function. The curve looks like a nonlinear analog signal. (c) The signal amplitude in the variation curve of (b) was divided into 32 linear levels to figure out the corresponding times of writing time for each level of the signal. (d) After irradiating for the given exposure times of wring light according to (b), the linear 32 levels of signal (NIR fluorescence at 720 nm) were achieved and read out by a reading light (680 nm). The quantized NIR signal is a type of digital signal.

experiments, 4-level, 16-level, 20-level, and 32-level models were proposed for demonstrating the capacity of multi-level optical storage. Firstly, the information recorded on the film can be completely erased by a 405 nm light (erasing light). Then, new information could be written using 621 nm irradiation (writing light). For most DTE derivatives, a long visible light wavelength irradiation could induce a 100% photocycloreversion reaction.[58,59] For DTE units, the open form has no absorption in the long wavelength region (Fig. S3†). There is a broad absorption peak of the closed-form DTE unit at around ~600 nm. That is because a relatively long wavelength could only induce the photocycloreversion but not the photocyclization reaction. In this work, the closed form TDI-4(DTE-TPE)-o under long visible light wavelength irradiation could be completely converted to open form. Thus, upon a relatively longer visible light wavelength (conservatively >500 nm), the DTE can induce the same photocycloreversion reaction yields of 100% (Fig. S7†). Choosing a different writing light wavelength does not change photocycloreversion reaction efficacy. This offers a broad range of alternatives for writing light wavelengths. In this work, we selected a 621 nm LED light to demonstrate the writing light function. The fluorescence intensities at 720 nm (fluorescence signal) are read out under 680 nm light (reading light) excitation to obtain the relationship between 621 nm light exposure and fluorescence intensity. Interestingly, the NIR intensity exhibited a great exponential relationship with the light exposure time (Fig. 5b). By correlating the NIR fluorescence signal amplitude with light exposure beforehand, we could transfer the nonlinear analog signal to a linear digital multi-level signal (Fig. 5c), which is suitable for computer-communication language. The maximum fluorescence intensity was divided into fixed equal levels and the exposure dose required for each stage was calculated based on the above relationship. Finally, $4(2^2)$, $16(2^4)$, $20(\sim 2^{4.3})$, and even $32(2^5)$ linear signal steps were obtained (Fig. 5d and S21–S23†), which is the first prototype of multi-level optical storage based on fluorescence photoswitching.

Significantly, a 32-level signal means a capacity of storage of 5-bit data per storage unit, which has dramatically improved the storage density (the commercial optical disc is 1 bit per storage unit). In the future, increasing the levels is possible to further improve the optical storage density based on higher-performance fluorescence photoswitching materials. The

 This journal is © The Royal Society of Chemistry 2023

Published on 07 February 2023. Downloaded on 12/4/2025 7:14:57 PM.

maximum divisible levels are principally dependent on (a) the destructive reading-out level (the reading light exposure will always cause a slow increase of fluorescence from the full closed state till the full open form is arrived), (b) the detection ability of the equipment (the lowest fluorescence signal amplitude of each stage can be resolved), (c) the precision control of light exposure as well as (d) the other related environment or equipment factors. The 32-level-optical storage described here is an example of multi-level storage based on fluorescence photoswitching. The levels of optical storage in a practical application would be mainly determined by the equipment condition and automatic fine control level if the ideal nonconstructive readout fluorescence photoswitching could be achieved in the future.

Unfortunately, the 680 nm irradiation led to a destructive readout of fluorescence (Fig. S24†). The fluorescence signal of the TDI-4(DTE-TPE)-pss sample was also gradually increased with reading time upon other irradiations such as 620 nm, 680 nm, 700 nm, and 720 nm (Fig. S25†). This deconstructive nature of the TDI-4(DTE-TPE) is mainly determined by the direct light absorption of closed-form DTE, the energy transfer caused by the partial overlaps of the absorption spectra of the closed-form DTE and the fluorescence spectra of TDI core[16] as well as the possibility of triplet–triplet energy transfer from TDI to the closed form DTE, which has been demonstrated in the literature.[60] The TDI core has a weak absorption above 700 nm, which is negligible above 730 nm (Fig. 2), which is not beneficial for capturing the fluorescence. Given these trade-offs, we employed the 680 nm light to read the fluorescence to guarantee a low deconstruction reading-out and a considerable fluorescence signal intensity. Although the absorption of closed-form DTE has weak absorption at that long wavelength, it offers an available process for photocycloreversion reaction. Nevertheless, the result gives us a suggestion that NIR fluorophore (such as quaterrylene imides) with the larger absorption wavelength and appropriate energy levels could be introduced into the photoswitching system in the future to achieve a complete nonconstructive reading out system without the energy transfer from NIR to DTE. Besides, the use of advanced narrow-band filters or monochromatic light sources and improving the control of light exposure are indispensable conditions of nondestructive readout.

3 Conclusions

In conclusion, a novel visible-light-driving solid-state NIR fluorescent bistable molecular switch was designed and synthesized by coupling AIE-gens TPE, photochromic DTE, and NIR emissive TDI into a single molecule. TPE, an electron-donating conjugation group, brings the visible light responsibility for the photocyclization reaction. As expected under 405 nm visible light irradiation, the fluorescence of TDI-4(DTE-TPE) was quenched by more than 93% and has good reversibility and fatigue resistance. TDI-4(DTE-TPE) has NIR emission at 786 nm in the solid state and the fluorescence intensity is 35 times higher than that of its precursor TDI powder. The relatively bright solid-state NIR fluorescence is due to the bulky substituent of TPE groups suppressing π–π stacking of TDI cores. The PMMA film of TDI-4(DTE-TPE) exhibits excellent fatigue resistance and stability under the condition of 85 °C and 85% humidity. The film was used as a optical storage medium to demonstrate a 32-level optical information storage prototype. The results show that photoswitchable NIR fluorescence molecules are a kind of potential photonic optical storage material. In the future, the optical storage medium with stronger solid-state luminescence efficiency and completely non-reconstructed readout-type photoswitching can be synthesized.

Author contributions

Conceptualization, C. Li and M.-Q. Zhu; funding acquisition, C. Li and M.-Q. Zhu; investigation, P. Hong, N.-H. Xie, K. Xiong, J. Liu, C. Li; methodology, C. Li, P. Hong, N.-H. Xie; project administration, C. Li and M.-Q. Zhu; resources, N.-H. Xie, K. Xiong; supervision, C. Li and M.-Q. Zhu; validation, P. Hong; visualization, P. Hong, C. Li; writing – original draft, C. Li and P. Hong, writing – review & editing, C. Li, P. Hong and M.-Q. Zhu.

Conflicts of interest

There are no conflicts to declare.

Acknowledgements

This work was supported by the National Key Research and Development Program of China (2021YFB2802004), the Knowledge Innovation Program of Wuhan-Basic Research (2022010801010086), the National Natural Science Foundation of China (NSFC 22275061, 22077037, 51673077) and the Fundamental Research Funds for the Central Universities (HUST: 2019KFYXKJC035). We thank Mr Kaiyuan Di from Wuhan National Laboratory of Optoelectronics (WNLO) of Huazhong University of Science and Technology (HUST) for the support of computational calculation. We also thank the Analytical and Testing Center of HUST, the Center of Optoelectronic Micro and Nano Fabrication and Characterizing Facility of WNLO (the engineer Dr Jun Su for SEM and TEM tests), and the Testing Facility of Energy Optoelectronics of WNLO for the use of their facilities.

References

1 L. Lu, K. Wang, H. Wu, A. Qin and B. Z. Tang, *Chem. Sci.*, 2021, **12**, 7058–7065.
2 H. Wang, X. Ji, Z. A. Page and J. L. Sessler, *Mater. Chem. Front.*, 2020, **4**, 1024–1039.
3 D. Okada, Z. H. Lin, J. S. Huang, O. Oki, M. Morimoto, X. Y. Liu, T. Minari, S. Ishii, T. Nagao, M. Irie and Y. Yamamoto, *Mater. Horiz.*, 2020, **7**, 1801–1808.
4 D. Xu, in *Multi-dimensional Optical Storage*, ed. D. Xu, Springer Singapore, Singapore, 2016, pp. 221–299, DOI: 10.1007/978-981-10-0932-7_4.
5 T. Liu, L. Zhang, J. Sun, Y. Zhong, Z. Wang, X. Guo and H. Ruan, *Zhongguo Jiguang*, 2018, **45**, 0903001.

Published on 07 February 2023. Downloaded on 12/4/2025 7:14:57 PM.

6 H. Hu, J. Pei, D. Y. Xu, G. S. Qi, H. Hu, F. S. Zhang and X. D. Liu, *Opt. Mater.*, 2006, **28**, 904–908.
7 Y. Qian, X. Xu, W. Li, J. Wang, B. Wei, Q. Wei, X. Yan, W. Hu, Y. Lu, L. Xie, X. Zhang and W. Huang, *Org. Electron.*, 2015, **26**, 476–480.
8 J. Jiang, P. Zhang, L. Liu, Y. Li, Y. Zhan, T. C. Wu, H. Xie, C. Zhang, J. Cui and J. Chen, *Chem. Eng. J.*, 2021, **425**, 131557.
9 T. Tsujioka, M. Kume and M. Irie, *Jpn. J. Appl. Phys.*, 1996, **35**, 4353.
10 G. S. Qi, J. X. Xiao, R. Liu, P. J. Jiang, P. She and D. Y. Xu, *Acta Physica Sinica*, 2004, **53**, 1076–1080.
11 H.-B. Cheng, S. Zhang, E. Bai, X. Cao, J. Wang, J. Qi, J. Liu, J. Zhao, L. Zhang and J. Yoon, *Adv. Mater.*, 2022, **34**, 2108289.
12 A. Mokhtar, R. Morinaga, Y. Akaishi, M. Shimoyoshi, S. Kim, S. Kurihara, T. Kida and T. Fukaminato, *ACS Mater. Lett.*, 2020, **2**, 727–735.
13 J. Zhang, B. He, Y. Hu, P. Alam, H. Zhang, J. W. Y. Lam and B. Z. Tang, *Adv. Mater.*, 2021, **33**, 2008071.
14 H. Al Sabea, L. Norel, O. Galangau, H. Hijazi, R. Métivier, T. Roisnel, O. Maury, C. Bucher, F. Riobé and S. Rigaut, *J. Am. Chem. Soc.*, 2019, **141**, 20026–20030.
15 C. Schörner, D. Wolf, T. Schumacher, P. Bauer, M. Thelakkat and M. Lippitz, *J. Phys. Chem. C*, 2017, **121**, 16528–16532.
16 N.-H. Xie, C. Fan, H. Ye, K. Xiong, C. Li and M.-Q. Zhu, *ACS Appl. Mater. Interfaces*, 2019, **11**, 23750–23756.
17 H. Tian and S. Yang, *Chem. Soc. Rev.*, 2004, **33**, 85–97.
18 C. Yun, J. You, J. Kim, J. Huh and E. Kim, *J. Photochem. Photobiol., C*, 2009, **10**, 111–129.
19 M. Irie, S. Kobatake and M. Horichi, *Science*, 2001, **291**, 1769–1772.
20 M. Morimoto, S. Kobatake and M. Irie, *Adv. Mater.*, 2002, **14**, 1027–1029.
21 T. Fumitaka, M. Masakazu and I. Masahiro, *Angew. Chem., Int. Ed.*, 2012, **51**, 901–904.
22 M. Berberich, M. Natali, P. Spenst, C. Chiorboli, F. Scandola and F. Würthnerr, *Chem. - Eur. J.*, 2012, **18**, 13651–13664.
23 T. Fukaminato, T. Doi, N. Tamaoki, K. Okuno, Y. Ishibashi, H. Miyasaka and M. Irie, *J. Am. Chem. Soc.*, 2011, **133**, 4984–4990.
24 S. Yamasaki, S. Ishida, S. Kim, M. Yamada, T. Nakashima, T. Kawai, S. Kurihara and T. Fukaminato, *Chem. Commun.*, 2021, **57**, 5422–5425.
25 L. Yuan, W. Lin, K. Zheng, L. He and W. Huang, *Chem. Soc. Rev.*, 2013, **42**, 622–661.
26 K. Uchida, M. Saito, A. Murakami, T. Kobayashi, S. Nakamura and M. Irie, *Chem. - Eur. J.*, 2005, **11**, 534–542.
27 T. Fukaminato, T. Doi, N. Tamaoki, K. Okuno, Y. Ishibashi, H. Miyasaka and M. Irie, *J. Am. Chem. Soc.*, 2011, **133**, 4984–4990.
28 A. Osuka, D. Fujikane, H. Shinmori, S. Kobatake and M. Irie, *J. Org. Chem.*, 2001, **66**, 3913–3923.
29 H.-y. Jung, B. Kim, M. H. Jeon and Y. Kim, *Small*, 2022, **18**, 2103523.
30 C. Wang, X.-K. Ma, P. Guo, C. Jiang, Y.-H. Liu, G. Liu, X. Xu and Y. Liu, *Adv. Sci.*, 2022, **9**, 2103041.
31 K. Jeong, S. Park, Y.-D. Lee, C.-K. Lim, J. Kim, B. H. Chung, I. C. Kwon, C. R. Park and S. Kim, *Adv. Mater.*, 2013, **25**, 5574–5580.
32 H. Kang, C. Fan, G. Liu and S. Pu, *Spectrochim. Acta, Part A*, 2019, **211**, 322–329.
33 L. Hou, R. Ringström, A. B. Maurer, M. Abrahamsson, J. Andréasson and B. Albinsson, *J. Am. Chem. Soc.*, 2022, **144**, 17758–17762.
34 M. Berberich and F. Wurthner, *Chem. Sci.*, 2012, **3**, 2771–2777.
35 T. Fukaminato, M. Tanaka, T. Doi, N. Tamaoki, T. Katayama, A. Mallick, Y. Ishibashi, H. Miyasaka and M. Irie, *Photochem. Photobiol. Sci.*, 2010, **9**, 181–187.
36 F. O. Holtrup, G. R. J. Müller, H. Quante, S. De Feyter, F. C. De Schryver and K. Müllen, *Chem. - Eur. J.*, 1997, **3**, 219–225.
37 Q. Qi, C. Li, X. Liu, S. Jiang, Z. Xu, R. Lee, M. Zhu, B. Xu and W. Tian, *J. Am. Chem. Soc.*, 2017, **139**(45), 16036–16039.
38 T. Fukaminato, T. Hirose, T. Doi, M. Hazama, K. Matsuda and M. Irie, *J. Am. Chem. Soc.*, 2014, **136**, 17145–17154.
39 C. Li, H. Yan, L. X. Zhao, G.-F. Zhang, Z. Hu, Z.-L. Huang and M.-Q. Zhu, *Nat. Commun.*, 2014, **5**, 5709.
40 C. Li, H. Yan, G.-F. Zhang, W.-L. Gong, T. Chen, R. Hu, M. P. Aldred and M.-Q. Zhu, *Chem. - Asian J.*, 2014, **9**, 104–109.
41 A. Eisfeld and J. S. Briggs, *Chem. Phys.*, 2006, **324**, 376–384.
42 Q. Zhao, J. Liu, H. Wang, M. Li, K. Zhou, H. Yang and Y. Han, *J. Mater. Chem. C*, 2015, **3**, 8183–8192.
43 L. Yang, Y. Yu, J. Zhang, F. Ge, J. Zhang, L. Jiang, F. Gao and Y. Dan, *Chem. - Asian J.*, 2015, **10**, 1215–1224.
44 T. Braeuniger, B. Groh, I. L. Moudrakovski and S. Indris, *J. Phys. Chem. A*, 2016, **120**, 7839–7846.
45 J. Vollbrecht, *New J. Chem.*, 2018, **42**, 11249–11254.
46 S. Benning, H. S. Kitzerow, H. Bock and M. F. Achard, *Liq. Cryst.*, 2000, **27**, 901–906.
47 J. Vollbrecht, C. Wiebeler, A. Neuba, H. Bock, S. Schumacher and H. Kitzerow, *J. Phys. Chem. C*, 2016, **120**, 7839–7848.
48 M. P. Aldred, C. Li, G.-F. Zhang, W.-L. Gong, A. D. Q. Li, Y. Dai, D. Ma and M.-Q. Zhu, *J. Mater. Chem.*, 2012, **22**, 7515–7528.
49 N.-H. Xie, C. Li, J.-X. Liu, W.-L. Gong, B. Z. Tang, G. Li and M.-Q. Zhu, *Chem. Commun.*, 2016, **52**, 5808–5811.
50 G.-F. Zhang, M. P. Aldred, W.-L. Gong, C. Li and M.-Q. Zhu, *Chem. Commun.*, 2012, **48**, 7711–7713.
51 M. Irie, K. Sakemura, M. Okinaka and K. Uchida, *J. Org. Chem.*, 1995, **60**, 8305–8309.
52 T. Sumi, Y. Takagi, A. Yagi, M. Morimoto and M. Irie, *Chem. Commun.*, 2014, **50**, 3928–3930.
53 H. Wu, L. Du, J. Luo, Z. Wang, D. L. Phillips, A. Qin and B. Z. Tang, *J. Mater. Chem. C*, 2022, **10**, 8174–8180.
54 Y. Dong, J. W. Y. Lam, A. Qin, Z. Li, J. Sun, H. H. Y. Sung, I. D. Williams and B. Z. Tang, *Chem. Commun.*, 2007, **1**, 40–42.
55 K. Singh Mehra, S. Jha, S. Bhandary, D. Mandal, R. Mishra and J. Sankar, *Angew. Chem., Int. Ed.*, 2022, **61**, e202205600.
56 M. Berberich, M. Natali, P. Spenst, C. Chiorboli, F. Scandola and F. Würthner, *Chem. - Eur. J.*, 2012, **18**, 13651–13664.

 This journal is © The Royal Society of Chemistry 2023

57 G. W. Zhang, J. H. Zheng, Z. X. Han and C. X. Tao, *Proc. SPIE 12066, AOPC 2021: Micro-optics and MOEMS*, Beijing, China, 2021.
58 M. Irie, T. Fukaminato, K. Matsuda and S. Kobatake, *Chem. Rev.*, 2014, **114**, 12174–12277.
59 T. B. Norsten and N. R. Branda, *Adv. Mater.*, 2001, **13**, 347–349.
60 T. Fukaminato, T. Doi, M. Tanaka and M. Irie, *J. Phys. Chem. C*, 2009, **113**, 11623–11627.

Published on 07 February 2023. Downloaded on 12/4/2025 7:14:57 PM.